Microsc. Microanal. 18, 699–704, 2012
doi:10.1017/S1431927612001237

Microscopy AND Microanalysis

© MICROSCOPY SOCIETY OF AMERICA 2012

Tuning Fifth-Order Aberrations in a Quadrupole-Octupole Corrector

Andrew R. Lupini[1,*] and Stephen J. Pennycook[1,2]

[1]*Materials Science and Technology Division, Oak Ridge National Laboratory, Oak Ridge, TN 37831, USA*
[2]*Department of Physics and Astronomy, Vanderbilt University, Nashville, TN 37235, USA*

Abstract: The resolution of conventional electron microscopes is usually limited by spherical aberration. Microscopes equipped with aberration correctors are then primarily limited by higher order, chromatic, and misalignment aberrations. In particular the Nion third-order aberration correctors installed on machines with a low energy spread and possessing sophisticated alignment software were limited by the uncorrected fifth-order aberrations. Here we show how the Nion fifth-order aberration corrector can be used to adjust and reduce some of the fourth- and fifth-order aberrations in a probe-corrected scanning transmission electron microscope.

Key words: aberrations, spherical aberration, higher order, STEM

Introduction

Aberration correctors are currently being used in many new high-resolution electron microscopes (for example, Haider et al., 2000; Dellby et al., 2001; Kisielowski et al., 2008; Sawada et al., 2010). These correctors generate negative third-order aberrations that cancel out the intrinsic positive, third-order, spherical aberration (C_s) of the round electron lenses (Scherzer, 1936). However, one potential drawback of a third-order corrector is that it can make other aberrations worse, in particular the chromatic (C_c) and higher-order aberrations (Rose, 1971) that can be difficult to directly control. To help combat these aberrations, most aberration correctors are now fitted with electron-optical elements that allow the coupling of the corrector to the objective lens to be altered. The possibility of using round lenses to reduce high-order terms was suggested several years ago (Rose, 1971) with detailed corrector designs proposed thereafter (Shao, 1988; Rose, 1990) and demonstrated in practice recently at 200 kV (Müller et al., 2006). The correction of these terms through the use of nonround elements (quadrupoles) has been implemented in the Nion UltraSTEM (Nion Company, Kirkland, WA, USA) (Dellby et al., 2008; Krivanek et al., 2008*a*, 2008*b*, 2008*c*). Here we briefly review a simple model for how these aberrations arise and demonstrate that correction of these terms is possible at both 60 and 100 kV, and that the measured values appear consistent over a period of about 2 years.

To illustrate both how fifth-order terms arise and how they can be corrected, we use a very simple model, based on that given by Shao (1988). Only propagation terms that arise between separated elements will be considered. It will be assumed that the angles are small and all other aberration terms will be neglected. This model assumes perfectly thin elements and rotational symmetry. For a more realistic model, computer simulation would normally be used instead. [It appears that manufacturers use their own in-house software, but for academic use TRANSPORT (Brown et al., 1983) provides calculations to third order and COSY INFINITY (Makino & Berz, 2005) appears to provide an interesting route to calculations of arbitrary order.] We will use the notation of Krivanek (e.g., Krivanek et al., 2008*b*), where aberrations are denoted by the letter C, with numerical subscripts that indicate the order of the aberration and then the rotation symmetry. Thus the third-order, round, spherical aberration (C_s) could also be written as C_{30}.

Figure 1 shows a schematic of an aberration corrector a distance L away from a lens. A ray traveling parallel to the axis at a distance r is deflected by the idealized, thin, aberration corrector. The objective lens then brings the ray to a focus after a distance f. If there are no aberrations, the ray will intersect the Gaussian focal point. For a lens with spherical aberration, the in-plane deviation X of the ray from the focal point is

$$X = C_s r^3/f^3. \tag{1}$$

If an aberration corrector is used to eliminate the spherical aberration, then the ray leaves the corrector at a slightly different angle α (see Fig. 1), meaning that instead of arriving at the lens at a position r, it arrives at $r + \alpha L$. Thus the angle after the thin lens will be $\alpha' = (r + \alpha)/f + C_s(r + \alpha)^3/f^4$ such that after propagating over a distance f and rearranging terms, the deviation from the focal point will be (see also Shao, 1988)

$$X = f\alpha - C_s r^3/f^3 + C_s(3r^2\alpha L + 3r\alpha^2 L^2 + \alpha^3 L^3)/f^3. \tag{2}$$

Thus if the deflection angle was chosen to be $\alpha = C_s r^3/f^4$, then the leading terms cancel (i.e., the spherical aberration is corrected), but the next term from equation (2) will leave a fifth-order aberration. The deviation for a round fifth-order spherical aberration C_{50} in this notation will be

$$X = C_{50} r^5/f^5. \tag{3}$$

Received March 15, 2012; accepted April 24, 2012
*Corresponding author. E-mail: 9az@ornl.gov; andy_lupini@hotmail.com

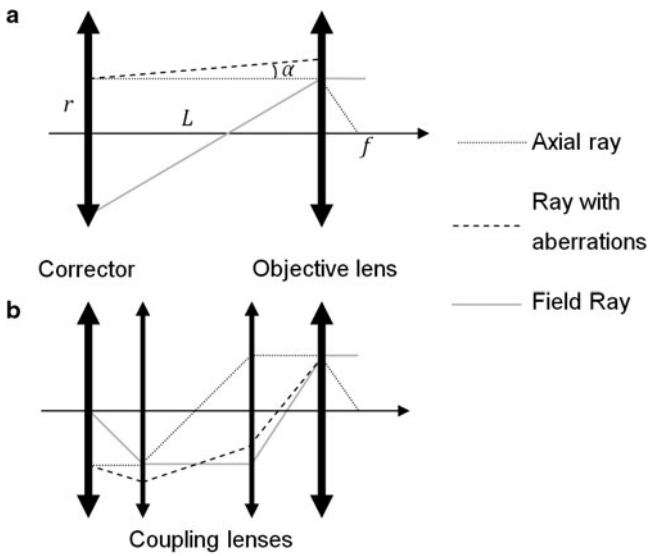

Figure 1. a: Simplified schematic of an aberration-corrected system (not to scale) showing how high-order aberrations arise because of the separation between the (ideal, thin) corrector and the (thin) objective lens. **b:** Adding coupling lenses provides control of the field rays and allows the propagation terms to be reduced.

Substituting the value for α into equation (2) gives

$$C_{50} = 3C_s^2 L/f^2. \tag{4}$$

In other words, correcting the C_s will usually cause additional higher order aberrations (Rose, 1971). Thus it may be worth deliberately setting a small amount of negative C_s to partially compensate for this aberration, as is often done in corrected HRTEM (Jia et al., 2010) or to compensate in some other way (Kirkland et al., 2006). However, a more direct route to eliminate the C_{50} is to change the distance L between the corrector and the objective lens. As it is not practical to physically adjust this length, the effective separation is changed using coupling lenses (Rose, 1971, 1990; Shao, 1988; Müller et al., 2006). The novel aspect in the Nion UltraSTEM used here is that the lenses are composed of a series of quadrupoles acting together (Dellby et al., 2008; Krivanek et al., 2008*c*).

Figure 1 also shows a schematic of the same aberration corrector with two extra lenses between the corrector and the lens (again following Shao, 1988 and Rose, 1990). Here it is assumed that these lenses are thin and that their contribution to the aberrations can be neglected. The lens strengths and spacings are chosen such that the ray that emerged from the corrector at a position r with an angle α appears at the objective lens with the same position and angle (both inverted). Effectively, these extra lenses are projecting the ray that leaves the corrector into the objective lens with no additional changes due to the propagation. Equivalently, the field rays are now constrained to have a crossover at the center of the corrector. In other words, the coupling optics are used to ensure that an arbitrary ray arrives at the "correct" part of the objective lens irrespective of r and α.

Clearly there are several other simplifications contained in the model of Figure 1. The diagram shows only one plane and other planes will be different with nonround elements (which shows that a similar argument will apply for nonround aberrations). In practice it might also be desirable to project the corrector into the objective lens in such a way that the phase change imparted by the corrector is magnified, which could be used to eliminate a large amount of C_s from a very poor lens (e.g., for Lorentz microscopy), or to run the corrector strongly and demagnify it in order to reduce parasitic effects. The main value of this model is that it demonstrates that the fifth-order aberrations of a third-order corrector can be adjusted by changing the coupling, rather than radical changes to the corrector itself. Practical designs to implement this principle were proposed by (Shao, 1988; Rose, 1990), and it was demonstrated in practice for round lenses and a hexapole-style corrector by Müller et al. (2006).

The fifth-order aberrations were one of the major limitations of the C_s-corrected VG Microscopes fitted with Nion aberration correctors. The C_s-corrected VG Microscopes' HB603 was able to resolve spacings to below 0.8 Å with evidence for information transfer to about 0.6 Å (Nellist et al., 2004) at 300 kV. Krivanek et al. (2008*a*) calculated the limiting aberration as about 60 mm of C_{54}, which would give a probe size limit of just below 0.5 Å and the precise values would depend upon the lens settings used. Since the VG Microscopes had two condenser lenses, which are carefully adjusted to set the source magnification and convergence angle, and very limited control of the coupling to the objective lens, there was little remaining flexibility to adjust the trajectory. Nominal values of the fifth-order aberrations would be measured only occasionally, while lower order terms of the corresponding symmetry would be routinely measured and adjusted to minimize the total contribution to the probe size. Discussion of the use of lower order terms to balance higher order aberrations in this way is given by Krivanek et al. (2008*b*, 2008*c*).

Materials and Methods

All results here were obtained using a Nion UltraSTEM operating at either 60 or 100 kV, as described by Krivanek et al. (2008*c*). In practice the C_{50} adjustment was made using a relatively high-level control in the Nion software that drives quadrupoles in layers 16-22 of the Nion corrector. The trajectories given by Krivanek et al. (2008*b*, 2008*c*) show the position of these coupling optics and describe the projection requirements in more detail. Although the actual adjustments consist of changing several quadrupoles and alignment coils, for our purposes this control can be compared to the action of the round coupling lenses in a hexapole style corrector. The advantages of using quadrupoles include lower power consumption and no rotation, but disadvantages include increased number of different power supplies to be adjusted.

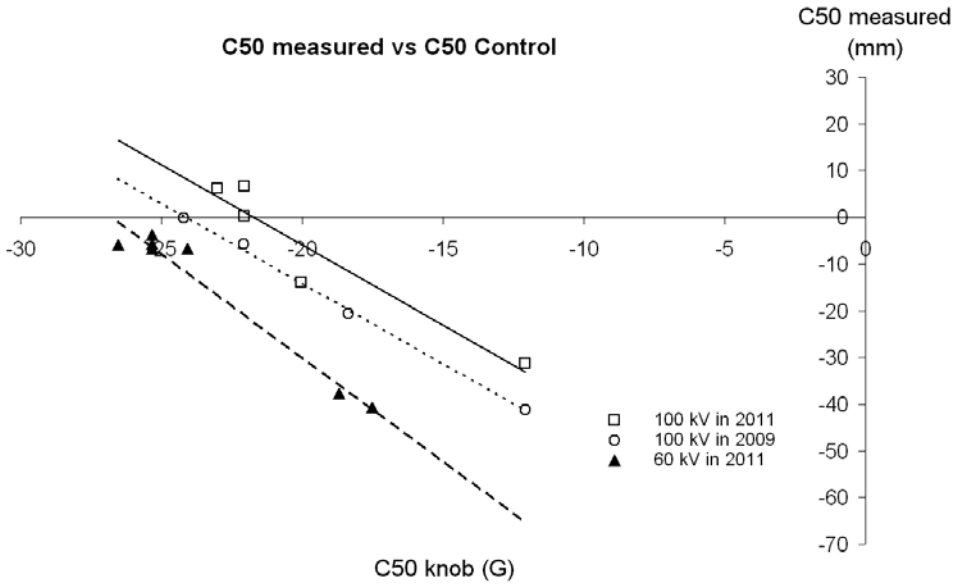

Figure 2. Measured C_{50} versus the C_{50} control knob at 100 kV in 2011 and 2009, and at 60 kV in 2011. Linear fits to the data are shown.

The procedure used was to measure the aberrations, adjust the control, then correct the misalignments that were introduced. Thus each measurement was the result of several iterations of adjusting the coupling quadrupoles, adjusting the octupole strengths to correct the third-order terms, then aligning the first- and second-order terms. The measurement itself was an iterative procedure because there is some cross talk between the aberrations of different orders. For example, large high order terms will introduce errors in the low-order aberrations, while large low-order aberrations will prevent accurate measurement of the high-order terms. In practice, as all aberrations converge, the errors introduced by this cross talk will decrease. Once the lower order aberrations were adequately corrected, then the higher order measurements were assumed to be reliable. The aberrations were measured using the Ronchigram analysis method described by Dellby et al. (2001).

Once the lower order aberration terms were corrected, the uncertainty in the C_{50} value was typically below 5 mm on any single measurement using the standard instrument settings. However, the use of a converging iterative procedure means that the final precision is the result of averaging several measurements at slightly different conditions each time, which should be better than a single measurement. To pursue higher resolution in future, the microscope software provides alternative options that could be used to make slower, but more accurate measurements.

Results

Figure 2 shows a plot of the measured round fifth-order aberrations with data from 2009 at 100 kV and 2011 at both 60 and 100 kV. At some time between the measurements, old settings files were loaded, undoing the correction. Although this action was undesirable, it allowed the repeatability of the adjustments to be examined. The repeated measurements have a very similar slope but different absolute values.

Figure 3 shows an example image of graphene taken at 60 kV in the Nion UltraSTEM after the correction procedure described here. The image shown is the sum of 20 fast frames (each about 1 s acquisition time) aligned by cross correlation and added, but is otherwise unprocessed. Since it is not completely clear whether this alignment might artificially boost the apparent resolution, we also verified that single-frame slow images acquired in the same session demonstrated a similar level of information transfer. The filtered Fourier transform demonstrates clear information transfer to 1.07 Å in all directions at 60 kV.

A related example showing the calculated probe size and the resolution that can be achieved in low-loss spectroscopy on graphene has recently been given by Zhou et al. (2011). There the probe full-width at half-maximum was calculated as approximately 1.01 Å at 60 kV, with a measured probe current of 110 pA.

Finally, Figure 4 shows the fourth- and fifth-order aberrations at 100 kV that were recorded during the correction process. The X-axis "Attempt" is used to indicate progression through the correction procedure. Note that each point is a single measurement of the higher order aberrations taken after several rounds of measurement and then correction of the lower order aberrations. Thus the data were chosen rather subjectively, and there are likely to be a variety of competing effects that contribute to these values. Table 1 shows some of the high-order aberrations measured at 60 kV after the correction process, along with the corresponding resolution limits from formulae given by Krivanek et al. (2008*a*), which are calculated under the assumption of the optimal aperture choice for each aberration independently.

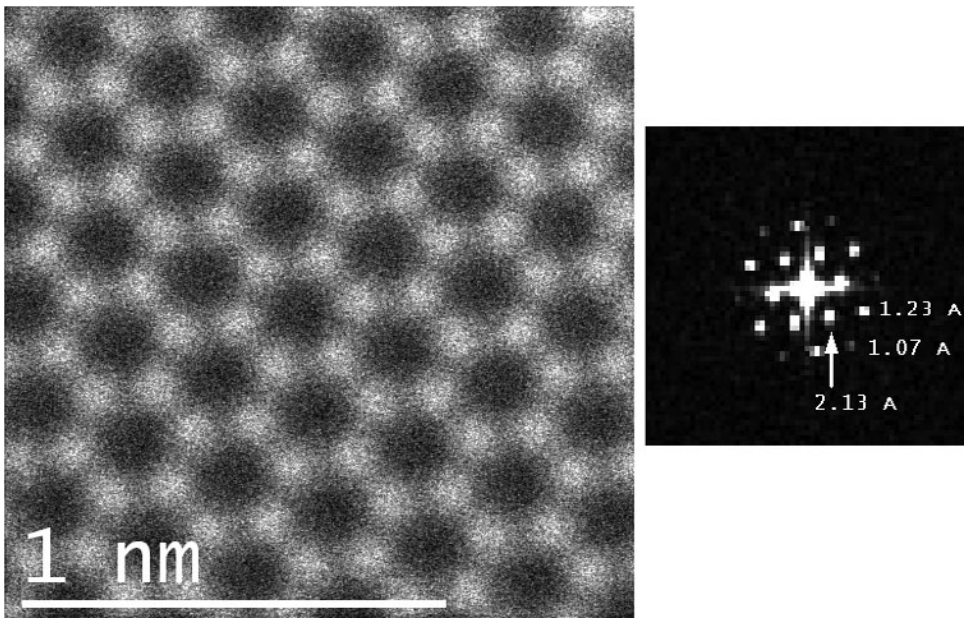

Figure 3. Scanning transmission electron microscope medium angle dark-field image of a single layer of graphene. This image is the sum of 20 fast frames aligned and summed, but is otherwise unprocessed. The filtered Fourier transform is shown on the right with information transfer to 1.07 Å at 60 kV.

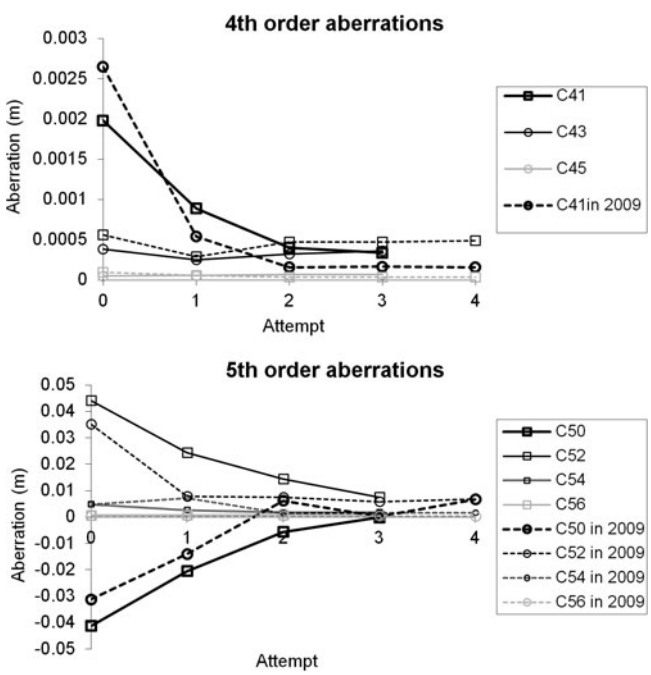

Figure 4. Fourth- and fifth-order aberrations at 100 kV as the C_{50} was reduced. For nonround terms, the modulus is plotted, i.e., $C_{52} = \sqrt{(C_{52a}^2 + C_{52b}^2)}$.

Discussion

Adjusting the coupling optics was found to provide a useful and relatively simple method to reduce the C_{50}. Having measurements from both 2009 and 2011 allows the repeatability of this process to be examined. The slope of the fitted lines gives the change in the measured aberration per change in the nominal C_{50} control and was about −3.4 mm/G at 100 kV in both cases. The similarity in the slope of the line fits would be expected because the C_s and focal length of the objective lens should be unchanged. Therefore, this similarity provides some confidence in the measured values and that the correction procedure will be repeatable. However, it is notable that the absolute values of C_{50} at the two dates are different by about 8.5 mm. Using nominal values of C_s = 1 mm and f = 1.5 mm (Dellby et al., 2008) in equation (4) would suggest that L changed by about 6 mm. Between those two experiments, the microscope had been significantly disassembled and rebuilt when it was moved to a new building, but it seems most likely that this change is due to different condenser lens settings after changing the field emission tip.

The line fit to the 60 kV measurements (−4.5 mm/G) was also found to be close to the 100 kV measurements. This similarity is perhaps a little artificial because the current outputs are scaled to their equivalent strength at the reference setting (100 kV for this instrument), i.e., the

Table 1. High-Order Aberrations Measured at 60 kV, and the Corresponding Probe-Size Limit Using the Formulae from Krivanek et al. (2008*a*).

Aberration	Value (m)	Probe Size (Å)
C_{50}	2.39E−04	0.33
C_{52}	1.69E−03	0.48
C_{54}	3.20E−03	0.63
C_{56}	9.21E−05	0.51
C_{41}	3.93E−04	0.71
C_{43}	6.39E−05	0.58
C_{45}	6.39E−05	0.87

currents flowing through the coils should really be regarded as "equivalent current at 100 kV" rather than "current." Similarly, the units (G) should also be taken as nominal strengths rather than measured fields. So it is perhaps surprising that there is any difference in slope between 60 and 100 kV. The uncertainty in the slopes was not calculated in detail, and trajectory differences will potentially affect the measurement. However, this different slope can most likely be attributed to the fact that the magnetic objective lens will be more saturated at 100 kV, and so the ratio of C_s/f is probably a little different at 60 kV.

In principle the C_{52} (twofold astigmatism of the fifth-order) terms could also be adjusted directly using the same method, by introducing astigmatism into the coupling optics. This was attempted here, but not investigated in detail because of the limited accuracy of the aberration measurement and the need to continually retune the lower order aberrations. In practice, reducing the C_{50} reduced the C_{52} terms close to the measurement accuracy. The major limitations were found to be the measurement accuracy and the rather extensive retuning of the lower order terms that was needed between iterations. The C_{54} terms remained small throughout the procedure (Fig. 4).

Given that the corrector eliminates the spherical aberration and that the coupling optics are used to reduce the fifth-order aberration, the next question will be what factors will then limit the resolution? Diffraction favors the choice of large beam limiting aperture θ because the diffraction limited probe size is

$$d_{diff} = 0.61\lambda/\theta. \tag{5}$$

For a wavelength of 4.87 pm at 60 kV, the nominal 30 mrad aperture corresponds to 0.99 Å, suggesting that the information limit apparent in Figure 3 is plausible. The probe size limit from chromatic aberration is Krivanek et al. (2008*b*)

$$d_{Cc} = 0.5(C_c \partial E/E)^{0.5} \text{ for an aperture size:}$$
$$\theta = 1.2(\lambda E/(C_c \partial E))^{0.5}. \tag{6}$$

Thus using $C_c \sim 1.3$ mm (Krivanek et al., 2008*a*) and $dE/E \sim 0.35/60{,}000$ for a cold field emission gun at 60 kV corresponds to a chromatic aberration limit of 0.96 Å for an optimal aperture of slightly larger than 30 mrad. The aperture size will also be limited by geometrical aberrations. The C_{50} contribution to the probe size is (Rose, 1981)

$$d_{50} = 0.4(C_{50}\lambda^5)^{1/6}. \tag{7}$$

Thus the initial value of ~50 mm would leave a resolution limit of 0.91 Å, but after the correction described here, a nominal residual value of 1 mm would give a resolution limit of 0.47 Å. Thus our procedure has shifted the C_{50} from a value where it is one of the most significant factors contributing to the probe size into the regime, where it is about a factor of 2 smaller than the chromatic contribution.

We used the formulae given by Krivanek et al. (2008*b*) to investigate which of the geometrical aberrations were giving a significant contribution to the resolution limit after correction. Using those formulae, the C_{50} limit would be slightly smaller than given above (0.42 Å for 1 mm), but they provide a good basis for an approximate comparison. Table 1 shows the results of an example measurement and the resulting probe size limits. Using those formulae, it appears that the fourth-order aberrations give a significant contribution to the probe size, even though they might be expected to be small in a quadrupole-octupole corrector. Although C_{45} was often the smallest fourth-order term (also see Fig. 4), the lack of lower order aberrations with the same symmetry means that it cannot be balanced by lower order terms, and so it contributed surprisingly strongly to the probe size limits. We did not extensively investigate the accuracy of the measured aberrations, and there might be some cross talk between the fitted aberrations. Since it appeared that more accurate adjustment was limited by the measurement noise, a more detailed examination of the precision to which the aberrations can be measured should be performed in future.

Conclusions

We have measured and corrected the fifth-order aberrations in a Nion UltraSTEM. The calibration given here should allow other users to correct the C_{50} of these instruments, and it will be interesting to see if the values found on other columns are similar. Once this correction is performed, the fifth-order adjustments are typically held constant and not changed again for several months. The method of C_{50} correction used in this machine is novel because it is achieved using quadrupoles instead of the more conventional round lenses. Reducing the fifth-order terms should produce a resolution improvement and in practice allowed an information limit of better than 1.07 Å at 60 kV to be achieved relatively easily on several samples.

We found that the fourth-order coma (C_{41}) was also reduced during the correction procedure (Fig. 4). A simple explanation is the hypothesis that those terms are due to similar propagation errors from the second-order coma (C_{21}). Therefore, optimizing the optical separation might be expected to reduce the fourth-order terms. The other two fourth-order terms were relatively unchanged during the correction procedure. Both the C_{43} and the C_{45} were small, which would be expected for an octupole corrector, and so any change would be hard to distinguish from the measurement noise.

We found that at 60 kV the most significant contribution to the resolution limit is the chromatic aberration. This could be reduced by going to higher accelerating voltages (as in Kisielowski et al., 2008*a*), monochromation (Tiemeijer et al., 2008; Krivanek et al., 2009), or C_c correction (Haider et al., 2008), when the residual fourth-order aberrations would become more significant.

Finally, it should be noted that this type of adjustment is not the only method to reduce the higher order aberrations. In practice a more complicated procedure, carefully measuring and adjusting the electron trajectories in each optical element is used to do a complete alignment (Kri-

vanek et al., 2008*a*). Similarly, adjusting the condenser lenses or objective lens might also allow the high-order aberrations to be changed. However, a full adjustment of the trajectories is a rather difficult and time-consuming exercise, while the above method is certainly suitable for making small improvements to the higher order aberrations that can be achieved by a general user in a relatively short time.

Acknowledgments

This research was supported by the U.S. Department of Energy, Basic Energy Sciences, Materials Sciences and Engineering Division. Technical assistance from Nion Co. is gratefully acknowledged. Graphene sample courtesy of H. Dai and T. Mirfakhrai of Stanford University, and additional microscopy courtesy of M.F. Chisholm and J. Guo.

References

Brown, K.L., Rothacker, F., Carey, D.C. & Iselin, Ch. (1983). TRANSPORT—A computer program for designing charged particle beam transport systems. SLAC-91, Rev. 3. Springfield, VA: National Technical Information Service, U.S. Department of Commerce.

Dellby, N., Krivanek, O.L. & Murfitt, M.F. (2008). Optimized quadrupole-octupole C_3/C_5 aberration corrector for STEM. *Phys Procedia* **1**, 179–183.

Dellby, N., Krivanek, O.L., Nellist, P.D., Batson, P.E. & Lupini, A.R. (2001). Progress in aberration-corrected scanning transmission electron microscopy. *J Elec Microsc* **50**(3), 177–185.

Haider, M., Müller, H., Uhlemann, S., Zach, J., Loebau, U. & Hoeschen, R. (2008). Prerequisites for a Cc/Cs-corrected ultrahigh-resolution TEM. *Ultramicroscopy* **108**, 167–178.

Haider, M., Uhlemann, S. & Zach, J. (2000). Upper limits for the residual aberrations of a high-resolution aberration-corrected STEM. *Ultramicroscopy* **81**, 163–175.

Jia, C.L., Houben, L., Thust, A. & Barthel, J. (2010). On the benefit of the negative-spherical-aberration imaging technique for quantitative HRTEM. *Ultramicroscopy* **110**, 500–505.

Kirkland, A.I., Meyer, R.R. & Shery Chang, L-Y. (2006). Local measurement and computational refinement of aberrations for HRTEM. *Microsc Microanal* **12**, 461–468.

Kisielowski, C., Freitag, B., Bischoff, M., Van Lin, H., Lazar, S., Knippels, G., Tiemeijer, P., Van Der Stam, M., Von Harrach, S., Stekelenburg, M., Haider, M., Uhlemann, S., Müller, H., Hartel, P., Kabius, B., Miler, D., Petrov, I., Olson, E.A., Donchev, T., Kenik, E.A., Lupini, A.R., Bentley, J., Pennycook, S.J., Anderson, I.M., Minor, A.M., Schmid, A.K., Duden, T., Radmilovic, V., Ramasse, Q.M., Watanabe, M., Erni, R., Stach, E.A., Denes, P. & Dahmen, U. (2008). Detection of single atoms and buried defects in three dimensions by aberration-corrected electron microscope with 0.5-Å information limit. *Microsc Microanal* **14**, 469–477.

Krivanek, O.L., Corbin, G.J., Dellby, N., Elston, B.F., Keyse, R.J., Murfitt, M.F., Own, C.S., Szilagyi, Z.S. & Woodruff, J.W. (2008*a*). An electron microscope for the aberration-corrected era. *Ultramicroscopy* **108**, 179–195.

Krivanek, O.L., Dellby, N., Keyse, R.J., Murfitt, M.F., Own, C.S. & Szilagyi, Z.S. (2008*b*). Advances in aberration-corrected scanning transmission electron microscopy and electron energy loss spectroscopy. In *Advances in Imaging and Electron Physics*, Hawkes, P.W. (Ed.), vol. 153, pp. 1–41. New York: Academic Press.

Krivanek, O.L., Dellby, N. & Murfitt, M.F. (2008*c*). Aberration correction in electron microscopy. In *Handbook of Charged Particle Optics*, 2nd ed. Boca Raton, FL: CRC Press.

Krivanek, O.L., Ursin, J.P., Bacon, N.J., Corbin, G.C., Dellby, N., Hrncirik, P., Murfitt, M.F., Own, C.S. & Szilagyi, Z.S. (2009). High-energy-resolution monochromator for aberration-corrected scanning transmission electron microscopy/electron energy-loss spectroscopy. *Phil Trans R Soc A* **367**, 3683–3697.

Makino, K. & Berz, M. (2005). COSY INFINITY Version 9. *Nucl Instrum Methods A* **558**, 346–350.

Müller, H., Uhlemann, S., Hartel, P. & Haider, M. (2006). Advancing the hexapole Cs-corrector for the scanning transmission electron microscope. *Microsc Microanal* **12**, 442–455.

Nellist, P.D., Chisholm, M.F., Dellby, N., Krivanek, O.L., Murfitt, M.F., Szilagyi, Z.S., Lupini, A.R., Borisevich, A.Y., Sides, W.H. & Pennycook, S.J. (2004). Direct sub-angstrom imaging of a crystal lattice. *Science* **305**, 1741–1742.

Rose, H. (1971). Abbildungseigenschaften spharish korrigierter elektronenoptischer Achromate. *Optik* **33**(1), 1–24.

Rose, H. (1981). Correction of aperture aberrations in magnetic systems with threefold symmetry. *Nucl Instrum Methods* **187**, 187–199.

Rose, H. (1990). Outline of a spherically corrected semiaplanatic medium-voltage transmission electron microscope. *Optik* **85**(1), 19–24.

Sawada, H., Sasaki, T., Hosokawa, F., Yuasa, S., Terao, M., Kawazoe, M., Nakamichi, T., Kaneyama, T., Kondo, Y., Kimoto, K. & Suenaga, K. (2010). Higher-order aberration corrector for an image-forming system in a transmission electron microscope. *Ultramicroscopy* **110**, 958–961.

Scherzer, O. (1936). Über einige Fehler von Elektronenlinsen. *Z Phys* **101**, 593–603.

Shao, Z. (1988). On the fifth-order aberration in a sextupole corrected probe-forming system. *Rev Sci Instrum* **59**, 2429–2437.

Tiemeijer, P.C., Bischoff, M., Freitag, B. & Kisielowski, C. (2008). Using a monochromator to improve the resolution in focal-series reconstructed TEM down to 0.5 Å. In *Proc. EMC 2008*, Aachen, Germany, Luysberg, M., Tillmann, K. & Weirich, T. (Eds.), vol. 1, pp. 53–54.

Zhou, W., Pennycook, S.J. & Idrobo, J.-C. (2011). Localization of inelastic electron scattering in the low-loss energy regime. *Ultramicroscopy* [Epub ahead of print]. Available at http://dx.doi.org/10.1016/j.ultramic.2011.11.013.